

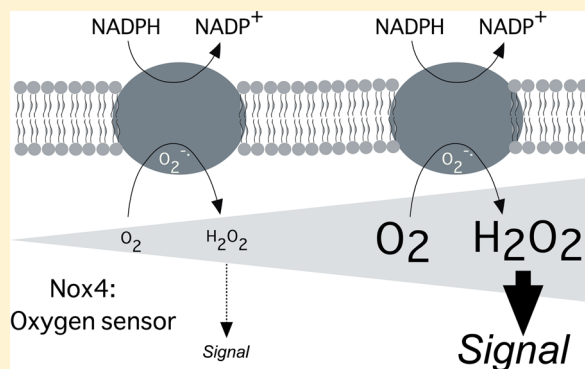
## Nox4: A Hydrogen Peroxide-Generating Oxygen Sensor

Yukio Nisimoto,<sup>†</sup> Becky A. Diebold, Daniela Cosentino-Gomes, and J. David Lambeth\*

Department of Pathology and Laboratory Medicine, Emory University Medical School, 148 Whitehead Building, 615 Michael Street, Atlanta, Georgia 30322, United States

### Supporting Information

**ABSTRACT:** Nox4 is an oddity among members of the Nox family of NADPH oxidases [seven isoenzymes that generate reactive oxygen species (ROS) from molecular oxygen] in that it is constitutively active. All other Nox enzymes except for Nox4 require upstream activators, either calcium or organizer/activator subunits (p47<sup>phox</sup>, NOXO1/p67<sup>phox</sup>, and NOXA1). Nox4 may also be unusual as it reportedly releases hydrogen peroxide (H<sub>2</sub>O<sub>2</sub>) in contrast to Nox1–Nox3 and Nox5, which release superoxide, although this result is controversial in part because of possible membrane compartmentalization of superoxide, which may prevent detection. Our studies were undertaken (1) to identify the Nox4 ROS product using a membrane-free, partially purified preparation of Nox4 and (2) to test the hypothesis that Nox4 activity is acutely regulated not by activator proteins or calcium, but by cellular pO<sub>2</sub>, allowing it to function as an O<sub>2</sub> sensor, the output of which is signaling H<sub>2</sub>O<sub>2</sub>. We find that approximately 90% of the electron flux through isolated Nox4 produces H<sub>2</sub>O<sub>2</sub> and 10% forms superoxide. The kinetic mechanism of H<sub>2</sub>O<sub>2</sub> formation is consistent with a mechanism involving binding of one oxygen molecule, which is then sequentially reduced by the heme in two one-electron reduction steps first to form a bound superoxide intermediate and then H<sub>2</sub>O<sub>2</sub>; kinetics are not consistent with a previously proposed internal superoxide dismutation mechanism involving two oxygen binding/reduction steps for each H<sub>2</sub>O<sub>2</sub> formed. Critically, Nox4 has an unusually high K<sub>m</sub> for oxygen (~18%), similar to the values of known oxygen-sensing enzymes, compared with a K<sub>m</sub> of 2–3% for Nox2, the phagocyte NADPH oxidase. This allows Nox4 to generate H<sub>2</sub>O<sub>2</sub> as a function of oxygen concentration throughout a physiological range of pO<sub>2</sub> values and to respond rapidly to changes in pO<sub>2</sub>.



Nox enzymes comprise a family of oxygen- and NADPH-dependent oxidoreductases that produce superoxide and/or hydrogen peroxide in a variety of cell types and tissues, often in response to hormones, growth factors, or immune mediators.<sup>1–3</sup> The classical NADPH oxidase, the Nox2 system, is strongly expressed in phagocytic cells such as neutrophils and macrophages in which the enzyme generates high levels of ROS as a major mechanism of antimicrobial host defense. Nox2, the catalytic subunit, is membrane-associated and binds to a second membrane protein, p22<sup>phox</sup>. The latter provides a proline-rich domain (PRD) that serves as a docking site for the “organizer” subunit p47<sup>phox</sup>,<sup>4</sup> which in turn binds to the activating subunit p67<sup>phox</sup>.<sup>5,6</sup> The small GTPase Rac also participates in activation<sup>7</sup> by binding to p67<sup>phox</sup>. Upon exposure of phagocytes to microbes or inflammatory mediators that act upon cell surface receptors, these components along with p40<sup>phox</sup><sup>8</sup> assemble at the membrane, triggered in part by phosphorylation of p47<sup>phox</sup> and GTP binding to Rac, resulting in activation of Nox2.

Nox1 and Nox3 but not Nox4 are regulated in a manner analogous to that of Nox2 involving regulatory subunits that are homologous to p47<sup>phox</sup> and p67<sup>phox</sup>.<sup>9–14</sup> Like Nox2, Nox1 is acutely activated by receptor-linked agonists (see, e.g., refs 15 and 16) and mediates various cellular responses, for example, in vascular smooth muscle and epithelial cells.<sup>3</sup> Acute regulation

of Nox3 is less well documented. While Nox1–Nox4 all require p22<sup>phox</sup>,<sup>13,17</sup> p22<sup>phox</sup> functions in a different manner for Nox4 for which the p22<sup>phox</sup> PRD docking domain is not required for binding to regulatory subunits but is needed for stability, perhaps conformational integrity, and/or maturation/localization.<sup>18–20</sup> Rather, Nox4 activity does not require regulatory subunits. Activation of Nox1–Nox3 but not Nox4 also requires the small GTPase Rac1.<sup>10,21,22</sup> Similarly, Nox5, Duox1, and Duox2 are all acutely activated by receptor-linked stimuli that elevate cellular calcium levels via their calcium-binding domains.<sup>23–25</sup>

Nox4 is expressed at its highest levels in the kidney<sup>26,27</sup> but is also widely expressed in many other cell types<sup>2</sup> and hence may have a cellular function that is more general than those of some other Nox enzymes whose tissue distributions are more restricted. For example, Nox3 is expressed almost exclusively in the inner ear where it functions in the development of otoliths.<sup>28</sup> The activity of Nox4 can be modestly stimulated by a DNA polymerase-interacting protein POLDIP2,<sup>29</sup> which was first suggested to regulate Nox1 and Nox4 on the basis of its

Received: March 18, 2014

Revised: July 23, 2014

Published: July 25, 2014

**Table 1. Partial Purification of His<sub>6</sub>-Nox4 Using Ni<sup>2+</sup>-Bead Affinity Chromatography<sup>a</sup>**

sample	total protein (mg)	heme (pmol/mg)	total heme (nmol)	specific activity [nmol of H <sub>2</sub> O <sub>2</sub> min <sup>-1</sup> (mg of protein) <sup>-1</sup> ]		purification (x- fold)	total activity (nmol of H <sub>2</sub> O <sub>2</sub> /min)	yield (%)
				without DPI	with DPI			
cell lysate	26	16	0.42	0.35	0.07	1	9.1	100.0
NEF/LSP	6.7	25	0.17	1.1	0.18	3.1	7.2	79
His <sub>6</sub> -Nox4	0.027	480	0.013	94	10	270	2.5	28

<sup>a</sup>NADPH-dependent hydrogen peroxide generating activity was measured by Amplex Red oxidation and heme content by oxidized-minus-reduced difference spectroscopy as detailed in Materials and Methods. Samples are those indicated in Figures 2 and 3 of the Supporting Information.

binding in a yeast two-hybrid screen to p22<sup>phox</sup>; however, the biological significance of this interaction is unclear, and Nox4 is not generally considered to be acutely regulated by subunit interactions. Rather, the most striking difference between Nox4 and other Nox/Duox enzymes is that Nox4 is constitutively active<sup>27,30</sup> in the absence of regulatory subunits or calcium-elevating stimuli. This has led to the concept that Nox4-dependent ROS generation is regulated primarily by its expression level.<sup>31,32</sup> This study explores the hypothesis that in addition to expression levels, the activity of Nox4 can be acutely regulated not by subunits or calcium but by tissue pO<sub>2</sub> and that its output of ROS serves as a signal that reports cellular oxygen levels.

The identity of the reactive oxygen product of Nox4 has been a matter of debate. Recent studies reported that the major product from Nox4 is H<sub>2</sub>O<sub>2</sub>,<sup>33</sup> although other studies (e.g., refs 27, 34, and 35) have detected superoxide. While some of the discrepancies may have resulted from the use of nonspecific assay reagents in detecting ROS,<sup>36–38</sup> some groups have suggested that the failure to detect superoxide results from membrane compartmentalization of Nox4-generated superoxide. While many Nox/Duox enzymes are localized at least in part at the cell surface where they can release their reactive oxygen product into the extracellular milieu, Nox4 is localized within the cell where it is reportedly localized to internal membranes such as the endoplasmic reticulum, nuclear membrane, and mitochondria.<sup>33,39–43</sup> While the exact subcellular location of Nox4 is controversial, association with any of these internal membranes is expected to direct reactive oxygen products into the membrane-enclosed cavity. Because superoxide is charged and unable to pass through lipid membranes while hydrogen peroxide is neutral and can readily traverse membranes and/or aquaporin channels, external probes should not detect the superoxide and would detect only hydrogen peroxide. According to this scenario, the cryptic superoxide dismutates within a membrane-limited cavity to form hydrogen peroxide, which escapes and is detected by ROS probes. To identify the ROS product of Nox4 in the absence of confounding membrane compartments, we have used a detergent-solubilized, partially purified preparation of Nox4.

## MATERIALS AND METHODS

**Materials.** Full-length cDNA encoding human Nox4 (amino acid residues 1–578) and N-terminally His<sub>6</sub>-tagged Nox4 were cloned into pcDNA 3.1 and pCIG vectors, respectively (Invitrogen). cDNA encoding N- or C-terminal His<sub>6</sub>-tagged full-length p22<sup>phox</sup> was cloned into pCIR (Invitrogen). The rabbit polyclonal antibody against a C-terminal synthetic peptide within the segment of amino acid residues 500–578 of human Nox4 was from Novus Biologicals,

Inc.; mouse monoclonal antibody 2366 to His<sub>6</sub> was from Cell Signaling Technologies, and mouse monoclonal antibody 44.1 against human p22<sup>phox</sup> was from Santa Cruz Biotechnology. Rabbit polyclonal antibodies to human lamin A (ab8980), calreticulin (ab4-100), and cadherin (ab6529-200) were obtained from Abcam. Goat anti-rabbit IgG and anti-mouse secondary antibodies linked to horseradish peroxidase were from Bio-Rad and Promega, respectively. Ni-NTA agarose was purchased from Qiagen, and amylose agarose and Factor Xa protease were from New England Biolabs. Protease inhibitor cocktail (EDTA-free) and Amplex Red were from Roche and Invitrogen, respectively. FAD, NADPH, diphenyleneiodonium (DPI), phenylmethanesulfonyl fluoride (PMSF), protein A-agarose Fast Flow [50% (v/v)], 3,3'-diaminobenzidine, and nuclei EZ lysis buffer were purchased from Sigma-Aldrich (St. Louis, MO). Percoll was from GE Healthcare Bio-Science AB. HEK293 cells stably transfected with Nox4 were the kind gift of R. P. Brandes (Goethe University, Frankfurt am Main, Germany). Micromat Gas tanks containing various oxygen/nitrogen mixtures were from Matheson Tri-Gas (Hilliard, OH).

**Transient Transfection of Nox4.** HEK293 cells were seeded at a density of 1 × 10<sup>6</sup> cells/plate (10 cm diameter) and grown for 24 h to 40–50% confluence in Dulbecco's modified Eagle's medium with 10% fetal serum, 100 units/mL penicillin, and 0.1 mg/mL streptomycin. Cells were transfected 48 h prior to use with mammalian expression vectors encoding Nox4, His<sub>6</sub>-Nox4, His<sub>6</sub>-Nox4(P437H), His<sub>6</sub>-p22<sup>phox</sup>, or empty vector, using FuGENE6 (Roche Molecular Biochemicals).

**Subcellular Fractionation by Differential Centrifugation.** Stable or transiently transfected HEK293 cells (typically ~1.5 × 10<sup>8</sup> cells) cultured in ~25 tissue culture plates (10 cm) were harvested, washed twice in PBS, suspended in nuclei EZ lysis buffer (pH 7.4) (Sigma-Aldrich) containing protease inhibitor cocktail (Complete Mini, Roche Diagnostics) with 0.2 mM PMSF, and disrupted using a glass homogenizer with a loose fitting pestle (3 min at 4 °C). The homogenate was centrifuged at 800g for 5 min in a Beckman TL-100 rotor at 4 °C to collect a nucleus-enriched fraction (NEF), and the supernatant was centrifuged at 10000g in a Beckman TL-100 rotor for 30 min to obtain the low-speed pellet (LSP). The supernatant (Sn) was centrifuged at 105000g for 60 min to yield the high-speed pellet (HSP) and the high-speed supernatant (HSS).

**Partial Purification of His<sub>6</sub>-Nox4.** From 25 to 30 mg of total lysate protein, the combined NEF and LSP were resuspended by homogenization on ice in buffer B [25 mM Hepes (pH 7.4) with 130 mM NaCl, 0.1 mM MgCl<sub>2</sub>, 10% glycerol, 1 μg/mL protease inhibitor cocktail, 0.5 mM PMSF, 20 μM FAD, 1% Nonidet P-40, and 0.2% deoxycholate] and then stirred gently for 30 min at 4 °C. The extract was centrifuged at 105000g for 60 min at 4 °C in a Beckman TL-

100 rotor, and the supernatant was applied to a Ni-NTA affinity column (10 mm × 15 mm) equilibrated with buffer B. The column was washed with 15 mL each of buffer B and then buffer B containing 10 mM imidazole. His<sub>6</sub>-Nox4 was eluted with buffer B containing 100 mM imidazole, and 0.2 mL fractions were collected. Fractions showing NADPH-dependent Amplex Red oxidizing activity were pooled, concentrated by Amicon Ultra-4 filtration, and dialyzed with two buffer changes against 250 mL of buffer B for 24 h at 4 °C to remove imidazole. The final material was characterized as described in Results and Discussion (Table 1 and Figure 4 of the Supporting Information).

**Isolation of Human Neutrophils.** Normal human neutrophils were obtained from peripheral blood of normal healthy donors after obtaining informed consent as described previously<sup>44</sup> and suspended in 0.9% saline at a density of 1–2 × 10<sup>8</sup> cells/mL. Human neutrophils were washed by centrifugation and resuspended in PBS (pH 7.4) containing 10 mM glucose.

**Preparation of Plasma Membrane and Cytosolic Fractions from Human Neutrophils.** After disruption of cells by sonication (3 × 5 s) on ice, cytosolic and plasma membrane-enriched fractions were separated by centrifugation at 105000g in a Beckman TL-100 rotor for 30 min at 3 °C using a Percoll density gradient as described previously<sup>45</sup> to obtain a plasma membrane-enriched fraction and a cytosolic fraction.

**Measurement of Superoxide.** Cytochrome *c* (final concentration of 100 μM) was added to a 0.8 mL cuvette containing 4.2 × 10<sup>5</sup> neutrophils in PBS (pH 7.4), and cells were activated at 25 °C with 0.12 μM PMA in the absence and presence of superoxide dismutase (300 units/mL). As described previously,<sup>46</sup> the rate of cytochrome *c* reduction was monitored for 10 min by the increase in absorption at 550 nm, monitored using an Ultraspec 3000 spectrophotometer (Pharmacia Biotech) and quantified using an extinction coefficient of 19.5 mM<sup>-1</sup> cm<sup>-1</sup> correcting for the low rate of cytochrome *c* reduction in the presence of SOD. Cytochrome *c* reduction by 2.1 × 10<sup>6</sup> Nox4-transfected cells was monitored using the same method, without activation by PMA. Neutrophil cell-free cytochrome *c* reductase activity was assayed in 0.8 mL of a reaction mixture consisting of PBS (pH 7.4), 20 μM GTPγS, 20 μM FAD, 100 μM NADPH, 100 μM cytochrome *c*, and 5 mM MgCl<sub>2</sub>, without or with 300 units/mL SOD, using 25 μg of protein of plasma membrane fraction with 0.2 mg of protein cytosol. The Nox2 system was activated by the addition of arachidonate (final concentration of 200 μM). Cytochrome *c* reduction by lysates or cell fractions from Nox4-expressing HEK293 cells in PBS (pH 7.4) containing 10 mM glucose was measured by the same method, except that the final cytochrome *c* concentration was 40 μM and GTPγS was omitted.

In some experiments, superoxide was also measured using dihydroethidium, according to ref 47 and using the same conditions that were used for cytochrome *c* reductase measurements.

**Measurement of Hydrogen Peroxide.** For intact cells, 100 μM Amplex Red final and 0.6 unit/mL HRP were included in place of cytochrome *c*, and the reaction was initiated by the addition of cells or fractions containing Nox4. The linear increase in the absorption of resorufin produced by oxidation of Amplex Red was measured at 572 nm.<sup>48</sup> For experiments monitoring fluorescence, respective excitation and emission wavelengths of 572 and 583 nm, respectively, were used for

cuvette measurements or fixed excitation and emission ranges of 540 ± 40 and 620 ± 40 nm, respectively, for microplate measurements. Reactions were monitored at 25 °C for 10 min using a Synergy 2 Multi-Model Microplate Reader and Gen 5, version 2.00 (Bio Tek), or, in oxygen dependence experiments, using a Pharmacia Biotec Ultraspec 3000 or a Hitachi F-4500 fluorescence spectrophotometer. For cell lysates, a final protein concentration of 0.25 mg/mL was added to a reaction mixture containing 20 μM FAD, 50 μM glucose 6-phosphate, and 50 μM NADP<sup>+</sup>. Endogenous glucose-6-phosphate dehydrogenase (G6PDH) was sufficient to support the NADPH oxidase reaction in lysates. For the isolated NEF/LSP cell fractions and for partially purified His<sub>6</sub>-Nox4, the same protocol was used, except that the indicated concentrations of enzyme or protein were added, and commercial G6PDH (0.25 unit/mL) was included. For cell-free measurements of Amplex Red oxidation, there is a well-documented<sup>49</sup> interference by reduced pyridine nucleotides. However, we have found that the inclusion of an NADPH-regenerating system consisting of glucose 6-phosphate and G6PDH, along with NADP<sup>+</sup>, markedly decreased the background rate. The remaining low residual rate of enzyme-independent Amplex Red oxidation was then subtracted to obtain corrected rates. The concentration of Amplex Red oxidized was calculated using an extinction coefficient at 572 nm of 54 mM<sup>-1</sup> cm<sup>-1</sup>,<sup>48</sup> or when fluorescence was measured using a standard curve generated from the addition of known amounts of hydrogen peroxide.

In some experiments, hydrogen peroxide was quantified using an Apollo 4000 Free Radical Analyzer (World Precision Instruments), equipped with a hydrogen peroxide electrode. The electrode system was used according to the manufacturer's instructions and allowed omission of HRP from assay mixtures.

**Regulation of the Oxygen Concentration.** The gas equilibration system consisted of a tightly capped 1.5 mL cuvette with a gas delivery needle and a gas exit needle that also served as a delivery port for addition of reagents. All experiments were conducted at 25 °C in a total volume of 0.8 mL. The mixture was equilibrated by gentle bubbling (approximately one bubble per second) with the indicated percent of oxygen/nitrogen gas mixtures, with continuous gentle stirring for 10 min using a magnetic stirrer. Concentrated stocks of activators (either PMA or arachidonate) were pre-equilibrated by being continuously bubbled with N<sub>2</sub> gas, and cells or cell fractions were activated by injecting 10 μL of activator through the gas exit needle with a 20 μL Hamilton syringe. Absorption, fluorescence, or luminescence measurements were taken as described above.

**Immunoprecipitation and Western Blot Analysis.** HEK293 cells were incubated in lysis buffer containing 1% Nonidet P-40 and 10% glycerol as described previously.<sup>30</sup> The mixture was gently mixed by rotation for 1 h at 4 °C with antibody (30 μg) against Nox4 with 25 μL of protein A-agarose Fast Flow beads (50% slurry). The beads were washed three times with lysis buffer, and bound proteins were eluted into 30 μL of Laemmli sample buffer (Bio-Rad). Proteins were separated via sodium dodecyl sulfate–polyacrylamide gel electrophoresis (4 to 15% gel) and transferred to an Immobilon PVDF membrane (Millipore). Proteins were visualized by being incubated with primary antibodies overnight at 4 °C with gentle shaking and then with horseradish peroxidase-linked secondary antibody (1:3000 dilution, 2 h). Bands were visualized by chemiluminescence after the addition of Super

Signal West Pico Chemiluminescent Substrate (Thermo Scientific), according to the manufacturer's instructions.

**Spectrophotometric Determination of Heme.** Solubilized cell lysate, combined NEF/LSP fractions, or partially purified proteins in buffer B were centrifuged at 105000g for 30 min at 4 °C to remove any particulate matter. Reduced-minus-oxidized difference spectra were recorded at 5 min intervals after the addition of a few crystals of sodium dithionite until a stable spectrum was achieved. The concentration of heme was determined from the difference spectrum near the Soret peak using a difference extinction coefficient at 426 minus 410 nm of  $200 \text{ mM}^{-1} \text{ cm}^{-1}$ .<sup>50</sup>

## RESULTS AND DISCUSSION

**Reactive Oxygen Product of Nox4.** Consistent with earlier publications, Figure 1A demonstrates that in intact HEK293 cells stably expressing Nox4, the major product is  $\text{H}_2\text{O}_2$  and very little superoxide is seen. In addition to the use of the Amplex Red method, this result was confirmed using a hydrogen peroxide electrode system. The electrode system reported approximately the same static concentrations of  $\text{H}_2\text{O}_2$  as did Amplex Red when cells were removed but detected a rate of hydrogen peroxide formation in the presence of cells that was approximately  $2/3$  of that of the Amplex Red method. This was presumably due to the “trapping” effect of HRP in the Amplex Red assay, which allows detection of all of the released  $\text{H}_2\text{O}_2$ , whereas the electrode measures a rate of  $\text{H}_2\text{O}_2$  that is decreased because of the competing metabolism by cellular catalase and peroxidases. This is in contrast to the case for neutrophils (Figure 1B), which express Nox2 but not other isoforms and show superoxide as the major product, with a smaller amount of  $\text{H}_2\text{O}_2$ , formed presumably as a dismutation product of superoxide. Superoxide detection reagents used in some earlier studies can be subject to certain artifacts such as nonselectivity for ROS/RNS and redox cycling that can artifactually generate superoxide,<sup>36–38</sup> and this has raised questions about the identity of the ROS product(s) generated by Nox4. Our superoxide measurements were taken using SOD-inhibited cytochrome *c* reduction, which, while less sensitive than methods based on fluorescence or luminescence, is considered to be a specific and reliable “gold standard”. Likewise, Amplex Red under controlled conditions is thought to reliably and quantitatively measure  $\text{H}_2\text{O}_2$ .<sup>48,51</sup> Thus, these data confirm an earlier report<sup>33</sup> that  $\text{H}_2\text{O}_2$  is the major Nox4 product elaborated by intact cells.

Similar results were seen in broken cell preparations of Nox4-expressing and control cells (Figure 1 of the Supporting Information), except that a higher background of cytochrome *c* reduction was seen that was only slightly inhibited by SOD. This is likely due to the presence of endogenous cytochrome *c* reductases such as P450 reductase for which cytochrome *c* reduction is not mediated by superoxide. In these preparations, there was no detectable difference in cytochrome *c* reduction in Nox4-expressing versus control cells. In contrast,  $\text{H}_2\text{O}_2$  was readily detected in Nox4-expressing but not control cells, with the  $\text{H}_2\text{O}_2$  identity validated by inhibition by catalase but not SOD (Figure 1 of the Supporting Information). Because of the very limited amounts of material available and the large volume needed for measurements using the  $\text{H}_2\text{O}_2$  electrode system, it was not feasible to use the electrode system for measurements in broken cell or purified preparations.

It can be argued that because of its transmembrane topology with its NADPH-binding site located on the cytosolic side of

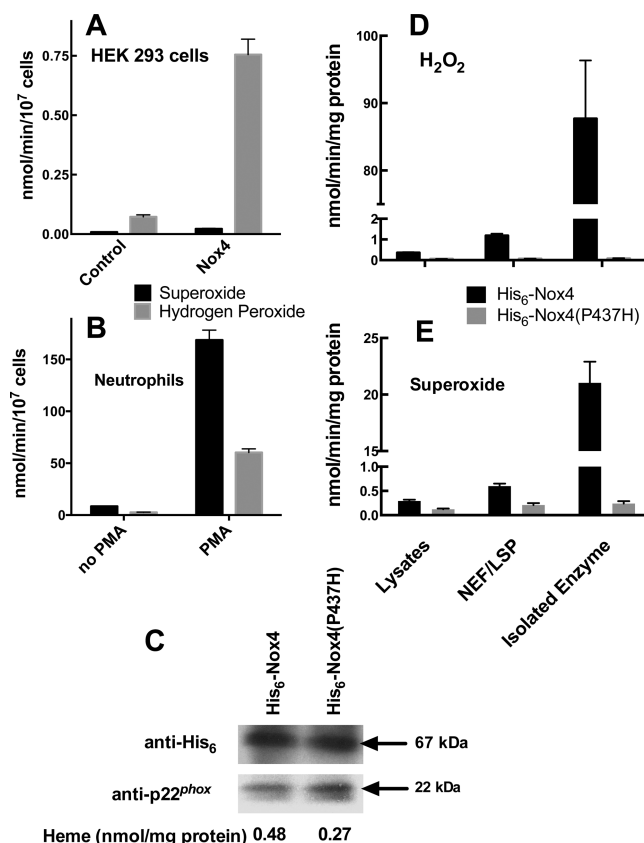


**Figure 1.** Hydrogen peroxide and superoxide generation by Nox4. (A) Hydrogen peroxide (gray bars) and superoxide (black bars) were measured in intact Nox4-expressing HEK293 cells as described in Materials and Methods. The reaction was initiated by adding  $5.25 \times 10^5$  cells to 0.8 mL of PBS (pH 7.4) containing 0.65 unit of HRP and 100  $\mu\text{M}$  Amplex Red to monitor  $\text{H}_2\text{O}_2$  generating activity. Superoxide generation was quantified as superoxide dismutase (SOD)-inhibited cytochrome *c* reduction, conducted in 0.8 mL of PBS (pH 7.4) containing 40  $\mu\text{M}$  cytochrome *c* with and without added SOD (final concentration of 300 units/mL). (B) Hydrogen peroxide (gray bars) and superoxide (black bars) were measured in isolated human neutrophils as described for panel A, using  $4.2 \times 10^5$  cells in 0.8 mL of PBS, and initiating the reaction with 0.12  $\mu\text{M}$  PMA. (C) Western blots of partially purified His<sub>6</sub>-Nox4 and His<sub>6</sub>-Nox4(P437H) were stained with antibody to His<sub>6</sub> or p22<sup>phox</sup>. The heme content of each preparation, determined by reduced-minus-oxidized difference absorption spectroscopy, is shown below the Western blot. (D) Hydrogen peroxide was quantified by Amplex Red oxidation in lysates, the combined NEF/LSP fraction, or the partially purified Nox4 from cells transfected with either His<sub>6</sub>-Nox4 (black bars) or His<sub>6</sub>-Nox4(P437H) (gray bars), as described in Materials and Methods. (E) Superoxide generation was measured by SOD-inhibited cytochrome *c* reduction in lysates, the combined NEF/LSP fraction, or the partially purified Nox4 from cells transfected with either His<sub>6</sub>-Nox4 (black bars) or His<sub>6</sub>-Nox4(P437H) (gray bars). Error bars represent the mean  $\pm$  SEM of three determinations using fractions from one transfection, and the experiment shown was repeated three times.

the membrane and the oxygen-reducing heme (heme B) located near the membrane-enclosed lumen, Nox4 might release superoxide into the interior of a membrane compartment where it is trapped due to its charge and therefore inaccessible to membrane-impermeant probes. There, it would be expected to undergo spontaneous and/or SOD-catalyzed dismutation to form  $\text{H}_2\text{O}_2$ . The latter might then diffuse through the membrane where it is detected by an extracellular

probe. Measurements made in both cell lysates and isolated membrane-containing cell fractions are also subject to the same theoretical concerns.

We therefore measured superoxide and hydrogen peroxide in a detergent-solubilized, partially purified preparation of Nox4 in which compartmentalization is not a concern. Details of the purification methods are provided in the Supporting Information and are summarized in Table 1. Briefly, cells and lysates from His<sub>6</sub>-Nox4-transfected cells were first verified to generate H<sub>2</sub>O<sub>2</sub> at a rate nearly the same as the rate of cells and lysates from cells transfected with wild-type Nox4, and H<sub>2</sub>O<sub>2</sub> generation was verified to be largely inhibited by the general flavoprotein dehydrogenase inhibitor diphenyleneiodonium (DPI) (Figure 2 of the Supporting Information). The NADPH-binding site mutant His<sub>6</sub>-Nox4(P437H), which is inactive, was used as a negative control and showed levels of H<sub>2</sub>O<sub>2</sub> generation nearly the same as those of nontransfected cells. Cells were fractionated by centrifugation and density methods into a nucleus-enriched fraction (NEF), a low-speed pellet (LSP), a high-speed pellet (HSP), and a high-speed supernatant (HSS), as shown in Figure 3 of the Supporting Information. Anti-His<sub>6</sub>, anti-Nox4, and anti-p22<sup>phox</sup> immunoreactivity was seen primarily in the NEF and LSP fractions, which also showed the highest level of DPI-inhibited H<sub>2</sub>O<sub>2</sub> production. These two fractions also stained for the nuclear marker Lamin A. While the colocalization of overexpressed Nox4 with nuclear markers does not definitively imply the nuclear localization of Nox4 in a natively expressing cell, it is interesting to note that Nox4 has been reported in several studies to be associated with nuclei;<sup>39,40</sup> nevertheless, other studies have reported localizations in other subcellular locations, including the endoplasmic reticulum, plasma membrane, and mitochondria.<sup>33,39,41–43</sup> NEF and LSP fractions were combined and used as a source for further purification using detergent solubilization followed by affinity chromatography on Ni<sup>2+</sup>-agarose, as shown in Figure 4 of the Supporting Information. The overall purification scheme is summarized in Table 1. The specific activity of the final preparation was enriched 270-fold over that of the starting material with an activity yield of 28%, based on DPI-inhibited H<sub>2</sub>O<sub>2</sub> generation. Heme enrichment was not used as an indicator of purification, because other endogenous heme proteins (e.g., cytochrome P450) may have been present in the less pure fractions. The final material showed a prominent band at 67 kDa (the predicted size of His<sub>6</sub>-Nox4) that was immunoreactive for both His<sub>6</sub> and Nox4 (Figure 4B of the Supporting Information). In addition, the preparation contained p22<sup>phox</sup> and heme (Figure 4 of the Supporting Information and Figure 1C).

In Figure 1, the generation of superoxide (panel E) and the generation of hydrogen peroxide (panel D) were compared in lysates, the combined NEF/LSP fractions, and the partially purified Nox4. Material isolated from cells transfected with the enzymatically inactive Nox4(P437H) was used to control for the possibility of artifactual co-isolation of other non-Nox4 ROS-generating activities. Approximately 80% of the product from the isolated Nox4 was detected as H<sub>2</sub>O<sub>2</sub>, whereas ~20% was detected as superoxide. The finding of both products may account for apparent discrepancies in the literature concerning the identity of the reactive oxygen species produced by Nox4, because both species are formed. Alternatively, a small superoxide signal may have been artifactually amplified through the use of redox cycling, superoxide-generating ROS detection probes in some studies. On the basis of the enzyme

concentration calculated from the heme content (assuming two hemes per Nox4 enzyme), ROS product formation corresponds to turnover numbers of 90 min<sup>-1</sup> for superoxide and 360 min<sup>-1</sup> for hydrogen peroxide. Because H<sub>2</sub>O<sub>2</sub> requires the two-electron reduction of oxygen whereas formation of superoxide requires only a single electron, this means that approximately 90% of the electron flux passing through the enzyme is directed toward the formation of H<sub>2</sub>O<sub>2</sub> and ~10% goes to form superoxide. Thus, isolated, detergent-solubilized His<sub>6</sub>-Nox4 forms primarily H<sub>2</sub>O<sub>2</sub>, with a small amount of released superoxide. This is consistent with the idea that superoxide is an intermediate in the formation of H<sub>2</sub>O<sub>2</sub> by Nox4 and that occasionally this intermediate is released and can be detected. Because the oxygen-reducing heme group is an obligate one-electron donor, a superoxide intermediate is mechanistically plausible, whereas the direct formation of H<sub>2</sub>O<sub>2</sub> without a superoxide intermediate is mechanistically implausible. It should be pointed out that the measured rate of turnover of Nox4 is only 10–20% of that of Nox2. While this value is still quite respectable (e.g., some P450 enzymes show rates below 10 min<sup>-1</sup>), we speculate that the rate of Nox2 that is much higher than that of Nox4 may represent an evolutionary adaptation to allow production of cytotoxic levels of H<sub>2</sub>O<sub>2</sub> for microbial killing, compared with the lower concentrations of H<sub>2</sub>O<sub>2</sub> that are likely to be needed for signal transduction.

**Oxygen Dependence of Nox4.** Herein, we explore the hypothesis that Nox4 activity is regulated not only by its expression level but also by oxygen availability and that it therefore functions as an oxygen sensor. For an enzyme to function as an oxygen sensor, it must fulfill two criteria. First, a *sine qua non* of an oxygen-sensing enzyme is an unusually high *K<sub>m</sub>* for oxygen that allows it to respond to physiological ranges of oxygen concentrations, which in tissues can range from 2–5% to around 20% in the lung, with intermediate concentrations in the circulatory system.<sup>52</sup> Second, its enzymatic activity must be linked to an effect or signal that can be translated into a cellular response. While Nox4 has been speculated to function in this manner,<sup>26,53,54</sup> the first of these criteria has not been previously evaluated. At least two oxygen-dependent enzymes, the HIF1- $\alpha$  prolyl hydroxylase PHD and the HIF1- $\alpha$  asparagine hydroxylase FIH-1, fit this paradigm and function as *bona fide* oxygen sensors, linked to the HIF1- $\alpha$ -dependent transcriptional response to hypoxia.<sup>55,56</sup> In both cases, the enzymes have high *K<sub>m</sub>* values for oxygen (10–20% O<sub>2</sub> for PHD and ~8% O<sub>2</sub> for FIH-1) that render the enzyme activity proportional to physiological ranges of tissue pO<sub>2</sub> values. Because hydroxylation by PHD targets HIF1- $\alpha$  for degradation and that by FIH-1 is inhibitory, the net effect of lowering pO<sub>2</sub> is to activate HIF1- $\alpha$ -dependent transcription. In contrast, oxygen-dependent enzymes (collagen prolyl hydroxylase, P450 enzymes, and cytochrome *c* oxidase) that participate in cellular functions unrelated to oxygen sensing show low *K<sub>m</sub>* values for O<sub>2</sub> (ranging from 0.2 to 3%), allowing them to function even at low to moderately low pO<sub>2</sub> values. While an enzyme with a low *K<sub>m</sub>* for oxygen will be nearly saturated at tissue levels of oxygen, a high *K<sub>m</sub>* for oxygen allows oxygen-sensing enzymes to respond in a nearly linear manner with respect to oxygen concentration. For example, if the oxygen concentration were to increase from 3 to 12%, Nox4 activity would increase ~300%. In contrast, an enzyme with an oxygen *K<sub>m</sub>* of 2% would increase its activity only ~25%. Thus, while a low *K<sub>m</sub>* allows an enzyme to function nearly optimally at

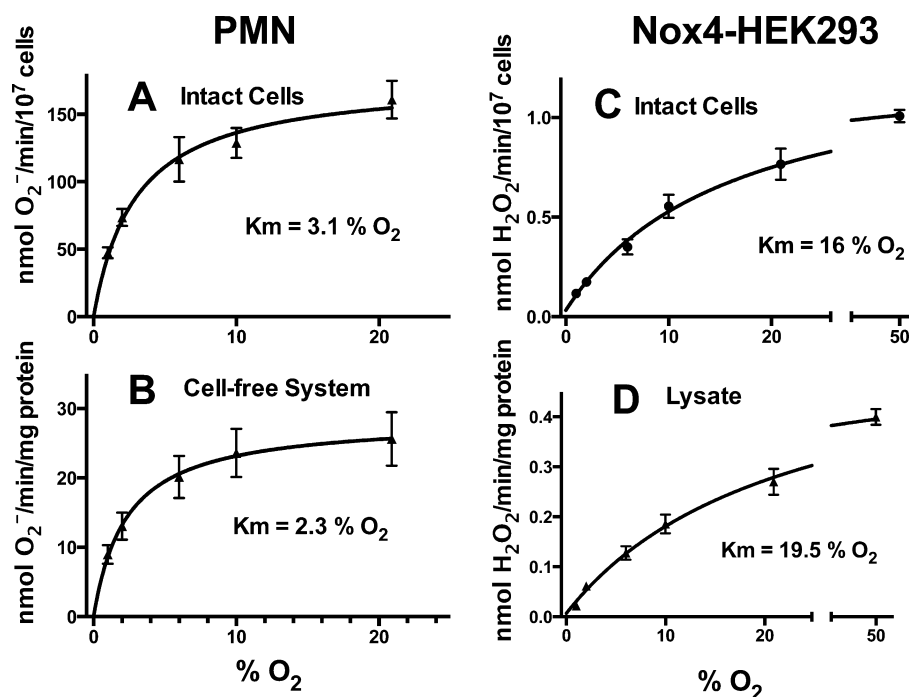


**Figure 2.** Oxygen concentration dependence for Nox2- and Nox4-dependent ROS generation. (A) Production of superoxide by intact human neutrophils was measured using superoxide dismutase-inhibited cytochrome *c* reduction as described in Materials and Methods. Human neutrophils ( $4.2 \times 10^5$ ) were suspended in 0.8 mL of PBS containing 100  $\mu\text{M}$  cytochrome *c* and equilibrated with  $\text{N}_2/\text{O}_2$  gas mixtures containing the indicated  $\text{O}_2$  percentage. Neutrophils were activated with a final PMA concentration of 0.12  $\mu\text{M}$ , added in 10  $\mu\text{L}$  from a 10  $\mu\text{M}$  stock that had been pre-equilibrated with 100%  $\text{N}_2$ , and the rate of cytochrome *c* reduction was measured. Cytochrome *c* reduction in the absence of PMA was negligible. (B) Superoxide production was quantified in a cell-free system from human neutrophils as detailed in Materials and Methods. After equilibration with the indicated gas mixtures at 25  $^\circ\text{C}$ , 8  $\mu\text{L}$  of a 20 mM archidonate stock that had been pre-equilibrated with 100%  $\text{N}_2$  was injected to give a final concentration of 200  $\mu\text{M}$ , and the rate of cytochrome *c* reduction was measured. (C)  $\text{H}_2\text{O}_2$  production by HEK293 cells stably expressing Nox4, measured using Amplex Red fluorescence as described in Materials and Methods. (D)  $\text{H}_2\text{O}_2$  production was monitored as described for panel C in lysates from Nox4-expressing HEK293 cells supplemented with FAD,  $\text{NADP}^+$ , and glucose 6-phosphate. Data points and error bars show the mean  $\pm$  SEM of three determinations from single experiments, and the experiments shown are representative of two or three. The solid lines in all panels show theoretical nonlinear least-squares fits of the data to the Michaelis–Menten equation, and the averaged  $K_m$  values are shown in each panel.

tissue  $\text{pO}_2$  values, it cannot respond dynamically to changes in  $\text{pO}_2$ ; in contrast, a high  $K_m$  enzyme operating at a subsaturating  $\text{pO}_2$  will change its activity dynamically with changes in  $\text{pO}_2$ .

The oxygen dependence for Nox2- versus Nox4-dependent ROS generation is compared in Figure 2. Nox2-dependent superoxide generation in either intact human neutrophils or a cell-free system shows a  $K_m$  for oxygen of 3.1 or 2.3%, respectively, corresponding to the range of  $K_m$  values seen in enzymes that participate in metabolic or cellular housekeeping functions. Because inflamed or infected tissues are often moderately hypoxic, this would allow the Nox2 system to continue to function at a significant rate under these conditions. On the other hand, Nox4 in both intact cells and lysates shows an oxygen  $K_m$  value for  $\text{H}_2\text{O}_2$  generation of 16–20%, corresponding to the  $K_m$  range seen for other known oxygen-sensing enzymes. Under our assay conditions, the rate of Nox4-dependent  $\text{H}_2\text{O}_2$  generation at both 21 and 1% oxygen was approximately linear for up to 3 h and was inhibited by DPI (data not shown). Because tissue oxygen concentrations are often on the order of 2–3%, this means that Nox4 will generate  $\text{H}_2\text{O}_2$  approximately in direct proportion to oxygen at concentrations below  $\sim 10\%$ , making it a sensitive reporter of tissue oxygenation.

**Mechanism of  $\text{H}_2\text{O}_2$  Generation.** Two mechanisms are possible for the generation of  $\text{H}_2\text{O}_2$  by Nox4. Because the FAD domain does not conduct this reaction directly,<sup>30</sup> both possible mechanisms require single electron transfers from heme to

oxygen. According to a “superoxide dismutase” mechanism that was previously suggested,<sup>33</sup> two superoxide molecules are formed in sequence and retained at the active site, and their sequestered dismutation before release from the enzyme results in  $\text{H}_2\text{O}_2$  formation. Such a mechanism is shown in Figure 3 (bottom), along with its rate equation. The oxygen dependence for such a mechanism involves two oxygen binding events and predicts a sigmoidal oxygen dependence, as shown by the dashed line in Figure 3. According to an internal superoxide reduction mechanism (Figure 3, top mechanism and rate equation), a single oxygen binds and is reduced in two sequential electron transfer steps from the heme, using a retained superoxide intermediate. Because there is a single oxygen binding event, such a mechanism predicts a simple hyperbolic Michaelis–Menten curve as shown by the solid black line in the top panel of Figure 3. Data replotted from Figure 2 show an excellent fit to the theoretical line predicted by a mechanism involving a single oxygen binding event for each  $\text{H}_2\text{O}_2$  formed (i.e., a mechanism in which sequential electrons are introduced into the oxygen from the heme), while they do not conform to the internal superoxide dismutation mechanism that would require two distinct oxygen binding events for each  $\text{H}_2\text{O}_2$  formed. Therefore, while either mechanism could account for a small production of superoxide (depending on the relative rate of dissociation compared with those of subsequent steps), kinetics are consistent only with a mechanism involving a single bound superoxide intermediate

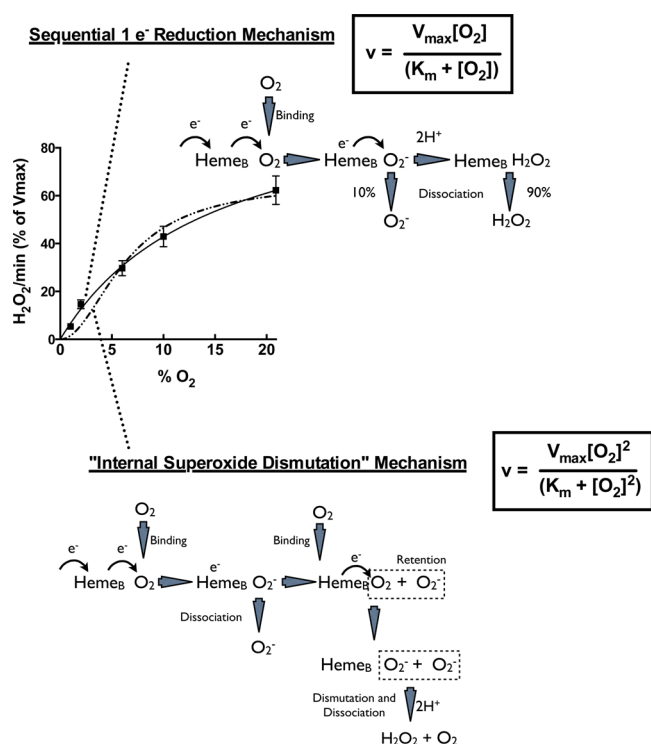


**Figure 3.** Analysis of the kinetic models for  $\text{H}_2\text{O}_2$  generation. Data from Figure 2D are replotted, normalized to the percentage of  $V_{\max}$ . The solid line was calculated from the kinetic rate equation corresponding to a “sequential one-electron reduction mechanism” (top equation and scheme), while the dashed line is that calculated from the equation corresponding to an “internal superoxide dismutation mechanism” (bottom equation and scheme). The former mechanism involves binding of a single oxygen, which is then reduced sequentially by heme B in two one-electron reduction steps. Depending on the rate of dissociation of superoxide compared with that of a second electron transfer step, the enzyme will release either superoxide or hydrogen peroxide. If the second electron transfer is more rapid than dissociation of the superoxide, then the primary product will be  $\text{H}_2\text{O}_2$ . The internal superoxide dismutation mechanism involves two discrete oxygen binding steps, each producing a superoxide at the active site. Both superoxide molecules are retained at the active site (indicated by the dashed box), and dismutation then results in the release of  $\text{H}_2\text{O}_2$ .

(termed a “sequential one-electron reduction mechanism” in Figure 3). Because such a mechanism has certain features in common with a superoxide reductase enzymatic activity, we also investigated the effects of azide and cyanide on  $\text{H}_2\text{O}_2$  and superoxide generation in Nox4-expressing cells. A bacterial superoxide reductase shows inhibition of the production of  $\text{H}_2\text{O}_2$  by these agents,<sup>57</sup> with accumulation of superoxide. The  $\text{H}_2\text{O}_2$  electrode system was used for hydrogen peroxide detection, because these agents inhibit the HRP that is needed in the Amplex Red assay. For superoxide, the DHE assay was used to allow for high sensitivity. While it was not possible to use cyanide using the electrode system because of signal instability, 0.6 mM sodium azide produced 70% inhibition of Nox4-dependent  $\text{H}_2\text{O}_2$  generation but did not cause any increase in superoxide production, suggesting that azide inhibits the overall Nox4 enzyme activity rather than a superoxide reduction step per se. Likewise, 1 mM KCN failed to increase superoxide generation in Nox4-expressing cells compared with that in control cells. Inhibition of Nox4 by azide is of interest in that Nox2 is not inhibited by azide or cyanide. Thus, azide

inhibition may point to differentiating features of the oxygen-binding heme site in Nox2 versus Nox4.

These data allow us to suggest a role for a critical histidine (His-222) residue for  $\text{H}_2\text{O}_2$  generation.<sup>33</sup> Mutation of this histidine, which is localized in an extracellular loop adjacent to heme B, converts Nox4 from a predominantly  $\text{H}_2\text{O}_2$ -generating enzyme to a predominant superoxide generator. We confirmed the switch to predominantly superoxide generation upon mutation of His-222 in intact cells (data not shown). On the basis of thermodynamic considerations, transfer of a second electron to the negatively charged  $\text{O}_2^{\bullet-}$  itself is energetically unfavorable, but donation of a histidyl proton to the  $\text{O}_2^{\bullet-}$  intermediate (bound at the heme B site) to form the neutral  $\text{HO}_2^{\bullet}$  should greatly facilitate transfer of a second electron, which (along with a solvent proton) forms  $\text{H}_2\text{O}_2$ . Mutation of this proton-donating histidine (which is absent in superoxide-generating Nox isoforms) should then favor release of superoxide rather than  $\text{H}_2\text{O}_2$ . We are currently investigating such a mechanism.

## SUMMARY

**Nox4 and Oxygen Sensing.** Nox4 was proposed to participate in oxygen sensing on the basis of its localization in kidney, which secretes the hormone erythropoietin in response to hypoxia.<sup>26</sup> Although the HIF-1 $\alpha$  system that regulates erythropoietin secretion had been proposed in earlier studies to respond to oxygen radicals, the oxygen-regulated enzymes prolyl hydroxylase and FIH-1 were subsequently discovered to be major regulators of the HIF-1 $\alpha$  system and Nox4 is not currently thought to be involved.<sup>55,56,58,59</sup> More recent studies have shown that responses of some ion channels to hypoxia require Nox4. The potassium channel TASK-1 is inhibited at 21% oxygen in Nox4-expressing cells (but not in Nox4-RNAi cells), and this inhibition is relieved by hypoxia.<sup>53</sup> Likewise, the activity of the smooth muscle ryanodine receptor  $\text{Ca}^{2+}$  release channel (RyR1) was oxygen-dependent and required Nox4, and the channel activity correlated with the oxidation of specific cysteine thiols in RyR1.<sup>54</sup> While these studies provide data consistent with an oxygen sensor role, the  $K_m$  of Nox4 for oxygen was not previously determined, and it was therefore not clear to us whether Nox4 was itself functioning as the oxygen sensor or was permissive in the response. These studies provide this missing information and show that Nox4 activity is responsive to physiological ranges of oxygen tension. This may be relevant in normal physiology, for example, in skeletal muscle,<sup>54</sup> wherein oxygen levels can dramatically and rapidly change with exercise. In addition, pathological ischemic conditions may also modulate Nox4 activity.

For an enzyme to function as an oxygen sensor, its enzymatic activity must be linked to a signal or an effector system that can mediate a downstream metabolic or cellular response.  $\text{H}_2\text{O}_2$  has long been implicated as a cellular signal and has been linked to a variety of cellular responses, including regulation of transcription, enzymatic activity, and ion channels.<sup>60–62</sup> In most signaling studies related to Nox enzymes, the cellular response is triggered by a receptor-linked hormone or growth factor that activates one of the Nox isoforms, rather than by oxygen concentration per se. Thus, the finding that Nox4 shows an unusually high  $K_m$  for oxygen and that it generates mostly hydrogen peroxide means that Nox4, rather than responding to external signals via intermediate signaling mechanisms such as changes in cellular calcium or phosphor-

ylation of regulatory subunits, responds directly and acutely to oxygen tension with the output of the signal molecule  $H_2O_2$ .

The role of Nox4 in oxygen sensing appears to be complex because oxygen levels can also regulate the expression of Nox4 itself. For example, the Nrf2 system transcriptionally induces antioxidant- and drug-metabolizing enzymes in response to oxidants and electrophilic compounds<sup>63,64</sup> as part of a pathway to adapt to cellular stresses. It is interesting that among the protein products induced by Nrf2 in response to hyperoxia is Nox4 itself, which may suggest that the induction of a Nox4-catalyzed  $H_2O_2$  signal is part of a cellular adaptation response to oxidative stress. In this context, adaptation to cellular stresses has previously been suggested as a general function for the Nox family of proteins.<sup>65</sup> Nox4 is also induced under hypoxic conditions in pulmonary artery smooth muscle cells via a HIF-1 $\alpha$  pathway,<sup>66</sup> suggesting that its regulation by oxygen may be complex and tissue-dependent. Nox4 is also induced by other stresses such as cardiac load-induced stress<sup>67</sup> and by inflammatory mediators via the NF- $\kappa$ B pathways<sup>68</sup> and in the former system has been shown to exert a beneficial effect, in contrast to the detrimental effect of Nox2 induction.<sup>67</sup> Thus, Nox4-derived  $H_2O_2$  may participate in signaling by both acute mechanisms dictated by the  $K_m$  of Nox4 for oxygen and by slower mechanisms involving the induction of Nox4 protein.

Regardless of the stimulus, induction of Nox4 would be expected to increase the magnitude of the response of Nox4 to oxygen concentration, further enhancing Nox4-dependent  $H_2O_2$  signaling with its consequent transcriptional induction of stress-adaptive proteins. We suggest that Nox4 is likely to participate in physiological processes, including adaptation to altitude and regulation of the delivery of oxygen to tissues, and that aberrant expression of Nox4 will lead to pathological processes, for example, related to the aberrant responses of tumors to hypoxia,<sup>69</sup> hypoxia-induced pulmonary hypertension,<sup>70</sup> and a growing list of diseases in which Nox4 has been implicated.<sup>71,72</sup>

In summary, Nox4 has been described as being unique among the Nox family of enzymes in that it is constitutively active without the need for external signals or regulatory proteins. Rather, these studies indicate that its activity is regulated acutely by oxygen tension. Its widespread distribution, including in cells of the vascular system, suggests important physiological roles for Nox4 in the rapid response to changes in oxygen tension in the circulatory system and in tissues. In this context, the primary output of the signaling molecule  $H_2O_2$  with minimal production of superoxide may allow for signaling with a level of production of toxic oxygen radicals lower than what would be possible with a superoxide-generating Nox isoform.

## ■ ASSOCIATED CONTENT

### ● Supporting Information

Four figures documenting the subcellular fractionation and characterization of Nox4-containing fractions and the partial purification of a membrane-free preparation of Nox4. This material is available free of charge via the Internet at <http://pubs.acs.org>.

## ■ AUTHOR INFORMATION

### Corresponding Author

\*E-mail: [noxdoc@mac.com](mailto:noxdoc@mac.com). Phone: (404) 727-5875.

### Present Address

<sup>†</sup>Y.N.: Visiting Professor, Department of Biomedical Sciences, College of Life and Health Sciences, Chubu University, 1200 Matsumoto-cho, Kasugai, Aichi 487-8501, Japan. E-mail: [ynisi4@isc.chubu.ac.jp](mailto:ynisi4@isc.chubu.ac.jp).

### Funding

Funded by National Institutes of Health Grant CA105116 and CNPq-Brazil (to D.C.-G.).

### Notes

The authors declare no competing financial interest.

## ■ ACKNOWLEDGMENTS

We thank Dr. Hisamitsu Ogawa (Department of Biology, Fujita Health University School of Medicine, Toyoake, Aichi, Japan) for the gift of wild-type and mutant His<sub>6</sub>-tagged Nox4 cDNA and Dr. Ralf Brandes (Center of Physiology, Goethe-University, Frankfurt, Germany) for providing the Nox4 stably expressing HEK293 cell line. We also thank Dr. Yeran Zhu and McCoy James (Department of Pathology and Experimental Medicine, Emory University Medical School) for technical assistance.

## ■ ABBREVIATIONS

ROS, reactive oxygen species; RNS, reactive nitrogen species; Nox, NADPH oxidase; PRD, proline-rich domain; NEF, nucleus-enriched fraction; LSP, low-speed pellet; Sn, supernatant; HSP, high-speed pellet; DPI, diphenyleneiodonium; PMSF, phenylmethanesulfonyl fluoride; FAD, flavin adenine dinucleotide; G6PDH, glucose-6-phosphate dehydrogenase; NADPH, nicotinamide adenine dinucleotide phosphate (reduced form); NADP<sup>+</sup>, nicotinamide adenine dinucleotide phosphate (oxidized form); PHD, HIF1- $\alpha$  prolyl hydroxylase; FIH-1, HIF1- $\alpha$  asparagine hydroxylase; SEM, standard error of the mean.

## ■ REFERENCES

- (1) Lambeth, J. D., Cheng, G., Arnold, R. S., and Edens, W. E. (2000) Novel homologs of gp91phox. *Trends Biochem. Sci.* 25, 459–461.
- (2) Cheng, G., Cao, Z., Xu, X., van Meir, E. G., and Lambeth, J. D. (2001) Homologs of gp91phox: Cloning and tissue expression of Nox3, Nox4, and Nox5. *Gene* 269, 131–140.
- (3) Lambeth, J. D. (2004) NOX enzymes and the biology of reactive oxygen. *Nat. Rev. Immunol.* 4, 181–189.
- (4) Ogura, K., Nobuhisa, I., Yuzawa, S., Takeya, R., Torikai, S., Saikawa, K., Sumimoto, H., and Inagaki, F. (2006) NMR solution structure of the tandem Src homology 3 domains of p47phox complexed with a p22phox-derived proline-rich peptide. *J. Biol. Chem.* 281, 3660–3668.
- (5) Iyer, S., Pearson, D., Nauseef, W., and Clark, R. (1994) Evidence for a readily dissociable complex of p47phox and p67phox in cytosol of unstimulated human neutrophils. *J. Biol. Chem.* 269, 22405–22411.
- (6) Han, C.-H., Freeman, J. L. R., Lee, T., Motalebi, S. A., and Lambeth, J. D. (1998) Regulation of the neutrophil respiratory burst oxidase: Identification of an activation domain in p67phox. *J. Biol. Chem.* 273, 16663–16668.
- (7) Diekmann, D., Abo, A., Johnson, C., Segal, A., and Hall, A. (1994) Interaction of Rac with p67phox and regulation of phagocytic NADPH oxidase activity. *Science* 265, 531–533.
- (8) Wientjes, F., Panayotou, G., Reeves, E., and Segal, A. (1996) Interactions between cytosolic components of the NADPH oxidase: p40phox interacts with both p67phox and p47phox. *Biochem. J.* 317, 919–924.
- (9) Geiszt, M., Lekstrom, K., Witta, J., and Leto, T. L. (2003) Proteins Homologous to p47phox and p67phox Support Superoxide Production by NAD(P)H Oxidase 1 in Colon Epithelial Cells. *J. Biol. Chem.* 278, 20006–20012.

- (10) Cheng, G., Diebold, B. A., Hughes, Y., and Lambeth, J. D. (2006) Nox1-dependent reactive oxygen generation is regulated by Rac1. *J. Biol. Chem.* 281, 17718–17726.
- (11) Cheng, G., Ritsick, D., and Lambeth, J. D. (2004) Nox3 regulation by NOXO1, p47phox, and p67phox. *J. Biol. Chem.* 279, 34250–34255.
- (12) Cheng, G., and Lambeth, J. D. (2005) Alternative mRNA splice forms of NOXO1: Differential tissue expression and regulation of Nox1 and Nox3. *Gene* 356, 118–126.
- (13) Kawahara, T., Ritsick, D., Cheng, G., and Lambeth, J. D. (2005) Point mutations in the proline-rich region of p22phox are dominant inhibitors of Nox1- and Nox2-dependent reactive oxygen generation. *J. Biol. Chem.* 280, 31859–31869.
- (14) Ueno, N., Takeya, R., Miyano, K., Kikuchi, H., and Sumimoto, H. (2005) The NADPH oxidase Nox3 constitutively produces superoxide in a p22phox-dependent manner: Its regulation by oxidase organizers and activators. *J. Biol. Chem.* 280, 23328–23339.
- (15) Suh, Y. A., Arnold, R. S., Lassegue, B., Shi, J., Xu, X., Sorescu, D., Chung, A. B., Griendling, K. K., and Lambeth, J. D. (1999) Cell transformation by the superoxide-generating oxidase Mox1. *Nature* 401, 79–82.
- (16) Lassegue, B., Sorescu, D., Szocs, K., Yin, Q., Akers, M., Zhang, Y., Grant, S. L., Lambeth, J. D., and Griendling, K. K. (2001) Novel gp91(phox) homologues in vascular smooth muscle cells: Nox1 mediates angiotensin II-induced superoxide formation and redox-sensitive signaling pathways. *Circ. Res.* 88, 888–894.
- (17) Ambasta, R. K., Kumar, P., Griendling, K. K., Schmidt, H. H., Busse, R., and Brandes, R. P. (2004) Direct interaction of the novel Nox proteins with p22phox is required for the formation of a functionally active NADPH oxidase. *J. Biol. Chem.* 279, 45935–45941.
- (18) Yu, L., Zhen, L., and Dinanuer, M. C. (1997) Biosynthesis of the phagocyte NADPH oxidase cytochrome b558. Role of heme incorporation and heterodimer formation in maturation and stability of gp91phox and p22phox subunits. *J. Biol. Chem.* 272, 27288–27294.
- (19) Nakano, Y., Banfi, B., Jesaitis, A. J., Dinanuer, M. C., Allen, L. A., and Nauseef, W. M. (2007) Critical roles for p22phox in the structural maturation and subcellular targeting of Nox3. *Biochem. J.* 403, 97–108.
- (20) Zhu, Y., Marchal, C. C., Casbon, A. J., Stull, N., von Lohneysen, K., Knaus, U. G., Jesaitis, A. J., McCormick, S., Nauseef, W. M., and Dinanuer, M. C. (2006) Deletion mutagenesis of p22phox subunit of flavocytochrome b558: Identification of regions critical for gp91phox maturation and NADPH oxidase activity. *J. Biol. Chem.* 281, 30336–30346.
- (21) Park, H. S., Lee, S. H., Park, D., Lee, J. S., Ryu, S. H., Lee, W. J., Rhee, S. G., and Bae, Y. S. (2004) Sequential activation of phosphatidylinositol 3-kinase,  $\beta$  Pix, Rac1, and Nox1 in growth factor-induced production of  $H_2O_2$ . *Mol. Cell. Biol.* 24, 4384–4394.
- (22) Ueyama, T., Geiszt, M., and Leto, T. L. (2006) Involvement of Rac1 in activation of multicomponent Nox1- and Nox3-based NADPH oxidases. *Mol. Cell. Biol.* 26, 2160–2174.
- (23) Edens, W. A., Sharling, L., Cheng, G., Shapira, R., Kinkade, J. M., Edens, H. A., Tang, X., Flaherty, D. B., Benian, G., and Lambeth, J. D. (2001) Tyrosine cross-linking of extracellular matrix is catalyzed by Duox, a multidomain oxidase/peroxidase with homology to the phagocyte oxidase subunit gp91phox. *J. Cell Biol.* 154, 879–891.
- (24) Geiszt, M., Witta, J., Baffi, J., Lekstrom, K., and Leto, T. L. (2003) Dual oxidases represent novel hydrogen peroxide sources supporting mucosal surface host defense. *FASEB J.* 17, 1502–1504.
- (25) Lambeth, D. O., Tews, K. N., Adkins, S., Frohlich, D., and Milavetz, B. I. (2004) Expression of two succinyl-CoA synthetases with different nucleotide specificities in mammalian tissues. *J. Biol. Chem.* 279, 36621–36624.
- (26) Geiszt, M., Kopp, J. B., Varnai, P., and Leto, T. L. (2000) Identification of renox, an NAD(P)H oxidase in kidney. *Proc. Natl. Acad. Sci. U.S.A.* 97, 8010–8014.
- (27) Shiose, A., Kuroda, J., Tsuruya, K., Hirai, M., Hirakata, H., Naito, S., Hattori, M., Sakaki, Y., and Sumimoto, H. (2001) A novel superoxide-producing NAD(P)H oxidase in kidney. *J. Biol. Chem.* 276, 1417–1423.
- (28) Banfi, B., Malgrange, B., Knisz, J., Steger, K., Dubois-Dauphin, M., and Krause, K. H. (2004) NOX3, a superoxide-generating NADPH oxidase of the inner ear. *J. Biol. Chem.* 279, 46065–46072.
- (29) Lyle, A. N., Deshpande, N. N., Taniyama, Y., Seidel-Rogol, B., Pounkova, L., Du, P., Papaharalambus, C., Lassegue, B., and Griendling, K. K. (2009) Poldip2, a novel regulator of Nox4 and cytoskeletal integrity in vascular smooth muscle cells. *Circ. Res.* 105, 249–259.
- (30) Nisimoto, Y., Jackson, H. M., Ogawa, H., Kawahara, T., and Lambeth, J. D. (2010) Constitutive NADPH-dependent electron transferase activity of the Nox4 dehydrogenase domain. *Biochemistry* 49, 2433–2442.
- (31) Krause, K. H. (2004) Tissue distribution and putative physiological function of NOX family NADPH oxidases. *Jpn. J. Infect. Dis.* 57, S28–S29.
- (32) Lambeth, J. D., Kawahara, T., and Diebold, B. (2007) Regulation of Nox and Duox enzymatic activity and expression. *Free Radical Biol. Med.* 43, 319–331.
- (33) Takac, I., Schroder, K., Zhang, L., Lardy, B., Anilkumar, N., Lambeth, J. D., Shah, A. M., Morel, F., and Brandes, R. P. (2011) The E-loop is involved in hydrogen peroxide formation by the NADPH oxidase Nox4. *J. Biol. Chem.* 286, 13304–13313.
- (34) Ago, T., Kitazono, T., Ooboshi, H., Iyama, T., Han, Y. H., Takada, J., Wakisaka, M., Ibayashi, S., Utsumi, H., and Iida, M. (2004) Nox4 as the major catalytic component of an endothelial NAD(P)H oxidase. *Circulation* 109, 227–233.
- (35) Ellmark, S. H., Dusting, G. J., Fui, M. N., Guzzo-Pernell, N., and Drummond, G. R. (2005) The contribution of Nox4 to NADPH oxidase activity in mouse vascular smooth muscle. *Cardiovasc. Res.* 65, 495–504.
- (36) Vasquez-Vivar, J., Martasek, P., Hogg, N., Karoui, H., Masters, B. S., Pritchard, K. A., Jr., and Kalyanaraman, B. (1999) Electron spin resonance spin-trapping detection of superoxide generated by neuronal nitric oxide synthase. *Methods Enzymol.* 301, 169–177.
- (37) Kalyanaraman, B. (2011) Oxidative chemistry of fluorescent dyes: Implications in the detection of reactive oxygen and nitrogen species. *Biochem. Soc. Trans.* 39, 1221–1225.
- (38) Maghazal, G. J., Krause, K. H., Stocker, R., and Jaquet, V. (2012) Detection of reactive oxygen species derived from the family of NOX NADPH oxidases. *Free Radical Biol. Med.* 53, 1903–1918.
- (39) Sturrock, A., Huecksteadt, T. P., Norman, K., Sanders, K., Murphy, T. M., Chitano, P., Wilson, K., Hoidal, J. R., and Kennedy, T. P. (2007) Nox4 mediates TGF- $\beta$ 1-induced retinoblastoma protein phosphorylation, proliferation, and hypertrophy in human airway smooth muscle cells. *Am. J. Physiol.* 292, L1543–L1555.
- (40) Kuroda, J., Nakagawa, K., Yamasaki, T., Nakamura, K., Takeya, R., Kuribayashi, F., Imajoh-Ohmi, S., Igarashi, K., Shibata, Y., Sueishi, K., and Sumimoto, H. (2005) The superoxide-producing NAD(P)H oxidase Nox4 in the nucleus of human vascular endothelial cells. *Genes Cells* 10, 1139–1151.
- (41) Van Buul, J. D., Fernandez-Borja, M., Anthony, E. C., and Hordijk, P. L. (2005) Expression and localization of NOX2 and NOX4 in primary human endothelial cells. *Antioxid. Redox Signaling* 7, 308–317.
- (42) Hilenski, L. L., Clempus, R. E., Quinn, M. T., Lambeth, J. D., and Griendling, K. K. (2004) Distinct subcellular localizations of Nox1 and Nox4 in vascular smooth muscle cells. *Arterioscler., Thromb., Vasc. Biol.* 24, 677–683.
- (43) Ago, T., Kuroda, J., Pain, J., Fu, C., Li, H., and Sadoshima, J. (2010) Upregulation of Nox4 by hypertrophic stimuli promotes apoptosis and mitochondrial dysfunction in cardiac myocytes. *Circ. Res.* 106, 1253–1264.
- (44) Boyum, A. (1968) Separation of leukocytes from blood and bone marrow. Introduction. *Scand. J. Clin. Lab. Invest., Suppl.* 97, 7.
- (45) Kjeldsen, L., Sengelov, H., and Borregaard, N. (1999) Subcellular fractionation of human neutrophils on Percoll density gradients. *J. Immunol. Methods* 232, 131–143.
- (46) Vermilion, J. L., Ballou, D. P., Massey, V., and Coon, M. J. (1981) Separate roles for FMN and FAD in catalysis by liver

microsomal NADPH-cytochrome P-450 reductase. *J. Biol. Chem.* 256, 266–277.

(47) Nazarewicz, R. R., Bikineyeva, A., and Dikalov, S. I. (2013) Rapid and specific measurements of superoxide using fluorescence spectroscopy. *J. Biomol. Screening* 18, 498–503.

(48) Rodrigues, J. V., and Gomes, C. M. (2010) Enhanced superoxide and hydrogen peroxide detection in biological assays. *Free Radical Biol. Med.* 49, 61–66.

(49) Votyakova, T. V., and Reynolds, I. J. (2004) Detection of hydrogen peroxide with Amplex Red: Interference by NADH and reduced glutathione auto-oxidation. *Arch. Biochem. Biophys.* 431, 138–144.

(50) Lutter, R., van Schaik, M. L. J., van Zwieten, R., Wever, R., Roos, D., and Hamers, M. N. (1985) Purification and partial characterization of the b-type cytochrome from human polymorphonuclear leukocytes. *J. Biol. Chem.* 260, 2237–2244.

(51) Mishin, V., Gray, J. P., Heck, D. E., Laskin, D. L., and Laskin, J. D. (2010) Application of the Amplex red/horseradish peroxidase assay to measure hydrogen peroxide generation by recombinant microsomal enzymes. *Free Radical Biol. Med.* 48, 1485–1491.

(52) Stroka, D. M., Burkhardt, T., Desbaillets, I., Wenger, R. H., Neil, D. A., Bauer, C., Gassmann, M., and Candinas, D. (2001) HIF-1 is expressed in normoxic tissue and displays an organ-specific regulation under systemic hypoxia. *FASEB J.* 15, 2445–2453.

(53) Lee, Y. M., Kim, B. J., Chun, Y. S., So, I., Choi, H., Kim, M. S., and Park, J. W. (2006) NOX4 as an oxygen sensor to regulate TASK-1 activity. *Cell. Signalling* 18, 499–507.

(54) Sun, Q. A., Hess, D. T., Nogueira, L., Yong, S., Bowles, D. E., Eu, J., Laurita, K. R., Meissner, G., and Stamler, J. S. (2011) Oxygen-coupled redox regulation of the skeletal muscle ryanodine receptor-Ca<sup>2+</sup> release channel by NADPH oxidase 4. *Proc. Natl. Acad. Sci. U.S.A.* 108, 16098–16103.

(55) Willam, C., Nicholls, L. G., Ratcliffe, P. J., Pugh, C. W., and Maxwell, P. H. (2004) The prolyl hydroxylase enzymes that act as oxygen sensors regulating destruction of hypoxia-inducible factor  $\alpha$ . *Adv. Enzyme Regul.* 44, 75–92.

(56) Kaelin, W. G., Jr., and Ratcliffe, P. J. (2008) Oxygen sensing by metazoans: The central role of the HIF hydroxylase pathway. *Mol. Cell* 30, 393–402.

(57) Shearer, J., Fitch, S. B., Kaminsky, W., Benedict, J., Scarrow, R. C., and Kovacs, J. A. (2003) How does cyanide inhibit superoxide reductase? Insight from synthetic FeIIIN4S model complexes. *Proc. Natl. Acad. Sci. U.S.A.* 100, 3671–3676.

(58) Berra, E., Benizri, E., Ginouves, A., Volmat, V., Roux, D., and Pouyssegur, J. (2003) HIF prolyl-hydroxylase 2 is the key oxygen sensor setting low steady-state levels of HIF-1 $\alpha$  in normoxia. *EMBO J.* 22, 4082–4090.

(59) Koivunen, P., Hirsila, M., Gunzler, V., Kivirikko, K. I., and Myllyharju, J. (2004) Catalytic properties of the asparaginyl hydroxylase (FIH) in the oxygen sensing pathway are distinct from those of its prolyl 4-hydroxylases. *J. Biol. Chem.* 279, 9899–9904.

(60) Hancock, J. T. (1997) Superoxide, hydrogen peroxide and nitric oxide as signalling molecules: Their production and role in disease. *Br. J. Biomed. Sci.* 54, 38–46.

(61) Schmidt, K., Amstad, K., Cerutti, P., and Baeuerle, P. (1995) The roles of hydrogen peroxide and superoxide as messengers in the activation of transcription factor NF- $\kappa$ B. *Chem. Biol.* 2, 13–22.

(62) Rohrdanz, E., and Kahl, R. (1998) Alterations of antioxidant enzyme expression in response to hydrogen peroxide. *Free Radical Biol. Med.* 24, 27–38.

(63) Lee, J. M., and Johnson, J. A. (2004) An important role of Nrf2-ARE pathway in the cellular defense mechanism. *J. Biochem. Mol. Biol.* 37, 139–143.

(64) Xie, T., Belinsky, M., Xu, Y., and Jaiswal, A. K. (1995) ARE- and TRE-mediated regulation of gene expression. Response to xenobiotics and antioxidants. *J. Biol. Chem.* 270, 6894–6900.

(65) Aguirre, J., and Lambeth, J. D. (2010) Nox enzymes from fungus to fly to fish and what they tell us about Nox function in mammals. *Free Radical Biol. Med.* 49, 1342–1353.

(66) Diebold, I., Petry, A., Hess, J., and Gorlach, A. (2010) The NADPH oxidase subunit NOX4 is a new target gene of the hypoxia-inducible factor-1. *Mol. Biol. Cell* 21, 2087–2096.

(67) Brewer, A. C., Murray, T. V., Arno, M., Zhang, M., Anilkumar, N. P., Mann, G. E., and Shah, A. M. (2011) Nox4 regulates Nrf2 and glutathione redox in cardiomyocytes in vivo. *Free Radical Biol. Med.* 51, 205–215.

(68) Manea, A., Tanase, L. I., Raicu, M., and Simionescu, M. (2010) Transcriptional regulation of NADPH oxidase isoforms, Nox1 and Nox4, by nuclear factor- $\kappa$ B in human aortic smooth muscle cells. *Biochem. Biophys. Res. Commun.* 396, 901–907.

(69) Hsieh, C. H., Chang, H. T., Shen, W. C., Shyu, W. C., and Liu, R. S. (2012) Imaging the impact of Nox4 in cycling hypoxia-mediated U87 glioblastoma invasion and infiltration. *Molecular Imaging and Biology* 14, 489–499.

(70) Lu, X., Murphy, T. C., Nanes, M. S., and Hart, C. M. (2010) PPAR $\gamma$  regulates hypoxia-induced Nox4 expression in human pulmonary artery smooth muscle cells through NF- $\kappa$ B. *Am. J. Physiol.* 299, L559–L566.

(71) Lambeth, J. D., Krause, K. H., and Clark, R. A. (2008) NOX enzymes as novel targets for drug development. *Semin. Immunopathol.* 30, 339–363.

(72) Krause, K. H., Lambeth, D., and Kronke, M. (2012) NOX enzymes as drug targets. *Cell. Mol. Life Sci.* 69, 2279–2282.

## NOTE ADDED AFTER ISSUE PUBLICATION

Author Daniela Cosentino-Gomes had her name spelled incorrectly in the version published on August 1, 2014. The revised version was published on the Web on August 18, 2014. An Addition and Correction was also published on August 18, 2014.